

mercially available equipment and time-lapse photography could be used.

There seems to be no reason why  $T_{in}$  should not appear for ions of higher specific energies than those investigated, although a higher etch temperature would be indicated, and the effect of increased etch temperature is one of the many variables that must be explored in the future. Another is the effect of variation of the entry angle. A preliminary measurement of the change in  $T_{in}$  when the angle was increased from  $41^\circ$  to  $51^\circ$  showed that it was reduced from 76 to 70 min in the case of the  ${}^6\text{Li}$  ion of 1.35 MeV/amu.

We wish to express our gratitude to Dr. H. C. Britt, group leader of P-9, Los Alamos Scientific Laboratory, Dr. W. G. Weitkamp, Technical Director, Nuclear Physics Laboratory, University of Washington, and Professor H. W. Lefevre, University of Oregon, and to their technical staffs, for their generous and expert assistance; to Dr. H. Bichsel of the University of Washington and to Dr. J. F. Dicello and Mr. S. D. Orbesen of Los Alamos Scientific Laboratory for their advice and help; and to S. C. Luckstead, R. C. Perry, S. T. Huber, A. S. MacArthur, and A. T. Brown of Washington State University for their indispensable and dedicated contributions to the initial work. Some support for this study was received from the Physics Department, the Nuclear Radiation Center, and the Graduate School of Washington State University, for which we are also very grateful.

<sup>1</sup>R. L. Fleischer, P. B. Price, and R. M. Walker, *Nuclear Tracks in Solids: Principles and Applications* (Univ. of California Press, Berkeley, 1975), Chap. 3, pp. 119–155.

<sup>2</sup>G. Baroni, S. Di Liberto, G. Romano, C. Sgarbi, and M. C. Tabasso, *Nucl. Instrum. Methods* **98**, 221 (1972).

<sup>3</sup>M. Monnin, thesis, University of Clermont, 1969, (unpublished), pp. 71–81.

<sup>4</sup>H. B. Lütck, *Nucl. Instrum. Methods* **131**, 105 (1975).

<sup>5</sup>The third coauthor (H.B.K.) was unable to observe the nascent tracks until they had been etched for about 5 min, but has since established that a correct phase contrast setup permits him to determine  $T_{in}$  much more precisely. The depth of the original etch bath prohibited the use of the proper (40×) phase contrast condenser, and so the 10× was used instead to give “modified phase contrast.”

<sup>6</sup>Ref. 1, p. 31.

<sup>7</sup>E. V. Benton, U. S. Naval Radiological Defense Laboratory, San Francisco, Report No. USNRDL-TR-67-80, 1967 (unpublished); E. V. Benton and R. P. Henke, University of San Francisco Technical Report No. 19, 1972, (unpublished).

<sup>8</sup>Ref. 1, p. 24, Eq. (1–6).

<sup>9</sup>Our  $(dE/dx)_{w < w_0}$  values were (indirectly) calculated from the stopping-power tables of L. C. Northcliffe and R. F. Schilling, [*Nucl. Data, Sect. A* **7**, 233 (1970)]. The lithium stopping-power values in these tables were obtained by interpolation and are thus considered to be less reliable than those for the other ions. However, it is unlikely that the calculated high-energy restricted energy losses can be very far from their correct values.

<sup>10</sup>Ref. 1, p. 41.

## Hydrodynamic Efficiency Measurements in Laser-Imploded Targets

I. Pelah,\* E. B. Goldman, and B. Yaakobi

*Laboratory for Laser Energetics, University of Rochester, Rochester, New York 14627*

(Received 26 April 1976)

We have found that numerical simulation and experiment both show laser-imploded spherical glass shells to expand in two successive pulses: The first corresponds to the ablated material, while the second corresponds to the compressed material. The relative speeds and intensities of the two pulses indicate the efficiency of transferring absorbed laser energy to the compressed core.

The laser energy necessary to achieve a gain  $M$  (fusion energy/laser energy) can be expressed<sup>1</sup> as  $E_L = 1.6M^3/C^2\epsilon^4$  MJ, where  $C$  is the compression and  $\epsilon$  is the efficiency of coupling laser energy to the compressed fusionable core. This coupling efficiency can be decomposed into two

parts:  $\epsilon_a$ , the absorption efficiency, and  $\epsilon_h$ , the hydrodynamic efficiency, defined as the fraction of absorbed energy which is transferred to the compressed core. Measurements of absorption efficiencies in the range of 10 to 80% have been reported<sup>2,3</sup> for various target and laser configura-

tions. On the other hand, no measurement of  $\epsilon_n$  has yet been published. We propose here a method for measuring the hydrodynamic efficiency via the ion current of the expanding pellet material. Although both experiment and numerical hydrodynamic-code simulation are found to substantiate the proposed method, systematic measurements have not been completed at this stage.

Charged-particle collectors placed at a distance  $L$  from a laser-irradiated target measure a pulse of ion current which typically rises to a maximum at a time corresponding to a velocity  $\approx 10^8$  cm/sec before decreasing. The measured current  $I(t)$  can be simply related to the density and velocity profiles in the target at any time  $t^*$  during the free expansion phase. Particles which at a time  $t^*$  were at a radius  $r$  will arrive at the detector at  $t = L/V(r, t^*)$  and give rise to a current

$$I(t) = 4\pi e r^2 N_e(r, t^*) V^2(r, t^*) / L V'. \quad (1)$$

Here  $V' = dV(r, t^*)/dr$  and the current of electrons or ions is integrated over the entire solid angle. In a steady state expansion the velocity is proportional to the radius so that  $I(t) \sim N_e(r, t^*) r^4$ . If we assume  $N_e(r, t^*) \sim \exp(-r/r_0)$  the resulting current will have a single peak at the velocity corresponding to  $r = 4r_0$ . However, peaks or even sharp changes in the slope of the density distribution may result in additional peaks in the current.

Using our one-dimensional hydrodynamic computer code (SUPER<sup>4</sup>) we performed simulations of spherical targets which do show such a second peak (except in the case of burnthrough of shells which results in negligible compression). As an example we summarize in Fig. 1 the results of the following computational experiment: a spherical glass shell of diameter 90  $\mu\text{m}$  and wall thickness 1  $\mu\text{m}$  filled with deuterium at 10 atm, total absorbed energy of 25 J delivered in a square (flat top) pulse of length 200 psec. In order to facilitate the presentation in one figure of a complete pellet evolution, we plot the results as a function of the Lagrangian radius, i.e., the horizontal scale is not proportional to the current distance from the center. The three curves correspond to three different times but all points on the same vertical line correspond to the same material point. The velocity is shown for the time at which the compression phase of the fuel dynamics has just been completed ( $t = 250$  psec). The inner part of the glass was still collapsing (negative velocity) when a strong shock reflected from the center expanded the gas fill. The combination of these motions gave rise to a dense thin layer,

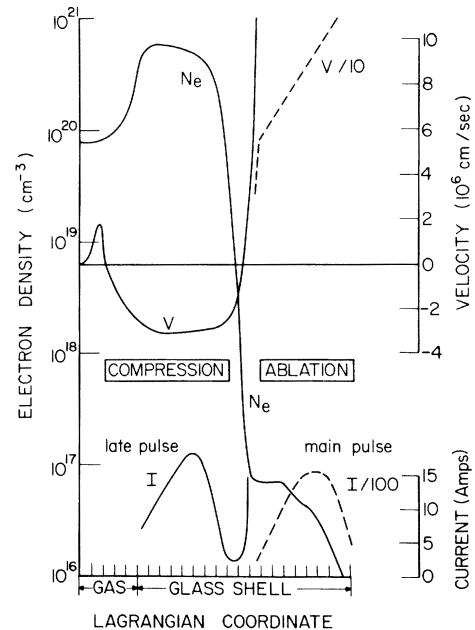


FIG. 1. Results from computer simulations for a glass spherical shell absorbing 25 J of laser energy (see text for details).  $V$  is the hydrodynamic velocity at  $t = 250$  psec,  $N_e$  is the electron density at  $t = 2.2$  nsec, and  $I$  is the current over the entire solid angle measured by a far detector. The Lagrangian radius is not proportional to the distance from the center.

which retained its relative shape for the rest of the expansion. This is clearly seen in the density profile at a much later time ( $t = 2.25$  nsec). Figure 1 also shows the computed contribution of each material point to the ion current at its time of arrival at a collector far from the pellet. This curve is related to the measured charged-particle collector signals if time runs (nonuniformly) to the left in Fig. 1; the actual time of arrival is given by the distance to the detector divided by the asymptotic velocity of the corresponding material shell. We see that the first (main) pulse corresponds to ablated material, whereas the second peak corresponds to material which had formed the compressed zone of the glass (along with the enclosed gas). Thus, the compressed pellet dynamics results in a density distribution which has two distinctly different slopes. This structure is frozen and leads, at much later times, to a double-humped shape in the ion current traces.

In these calculations the energy absorbed is adjusted to a given value; part of the available energy is absorbed by inverse bremsstrahlung and the rest is deposited at the critical layer. Heat conduction is assumed to be classical and unin-

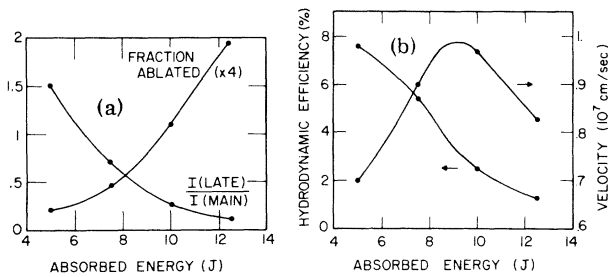


FIG. 2. Results from computer simulations for different absorbed energies (see text for details). (a) Fraction of glass shell which is ablated and ratio of total charge in the late and main ion pulses. (b) Velocity of the late ion pulse and its relative energy, or the hydrodynamic efficiency.

hibited. Local charge is determined by solving the coupled rate equations describing ionization and recombination of the various target species.<sup>5</sup> The main ion current pulse arrives at the collector almost totally ionized, while the late pulse is predicted to be in a lower charge state, in agreement with a direct measurement.

Inspection of the computed pellet behavior shows that the kinetic energy of collapse is converted to thermal energy of the fuel and back to kinetic energy of expansion with little loss to radiation or to acceleration of outer layers. The measured energy in the late ion pulse is therefore essentially equal to the hydrodynamic energy available for compression.

Figure 2 summarizes the results of computer calculations for conditions similar to those in Fig. 1, except with varying absorbed energy. As is seen, the relative (time-integrated) intensity of the late ion pulse decreases with increased energy, Fig. 2(a), but the corresponding velocity and energy show a pronounced maximum. The hydrodynamic efficiency decreases monotonically, but the hydrodynamic energy itself (product of efficiency and absorbed energy) reaches a maximum of 0.4 J when  $\sim \frac{1}{8}$  of the glass shell is ablated; less ablation produces a smaller pressure, whereas more ablation leaves relatively less material to act as a tamper. Finally we show in Fig. 3(a) the calculated history of ion current over the entire solid angle at a distance 25 cm from the target for an absorbed energy 10 J. The late current peak in Fig. 3(a) contains both ionized and neutral material, both of which should be detected for a determination of the hydrodynamic energy. Here, current corresponds to charge flux and neutrals have been arbitrarily assigned a unit charge.

Experiments have been performed with target

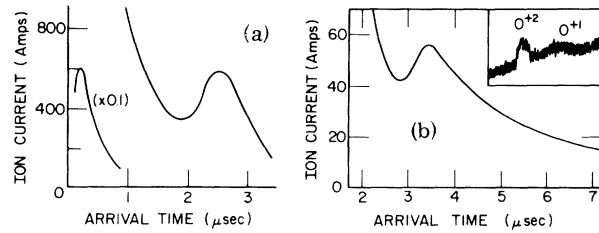


FIG. 3. Comparison of the calculated (a) and measured (b) late ion pulse for a glass microballoon target absorbing 10 J of laser energy. Current is over the entire solid angle. The ion current detector in both cases is at a distance 25 cm from the target. Inset: trace of a single-detector constant-voltage mass spectrometer. The arrival time of the O<sup>+2</sup> and O<sup>+1</sup> peaks correspond to the rising and falling portions of the late ion pulse, respectively.

and laser parameters similar to those in Fig. 2. More details on our four-beam laser system and diagnostic methods may be found in Ref. 2. Most experiments indeed produced a late ion pulse as predicted. In addition, the main pulse was in many cases preceded by the clearly differentiated, so-called fast ion component. For absorbed energy in the range 5–10 J, the velocity of this pulse varied in the range  $(0.6-1) \times 10^7$  cm/sec, in good agreement with Fig. 2(b). Figure 3(b) is an example of the measured ion current for a shot with about 10 J absorbed energy. When a lower gain was used in measuring the current, the main ion pulse could be seen to peak at 0.3 μsec. The charge collector was placed at a distance 25 cm from the target and its output was normalized to the entire solid angle assuming complete isotropy. The agreement in the time of appearance of the late pulse in Figs. 3(a) and 3(b) is satisfactory in view of the uncertainty ( $\approx 20\%$ ) in the measurement of absorbed energy. In fact, if the absorbed energy were actually 14 J, the numerical results of Fig. 3(a) would predict correctly the late pulse velocity [Fig. 3(b)], and would overestimate its total charge by about a factor of 2. This overestimate is due to the neutrals not detected in the present arrangement. The reason for the low ionization state of the late peak is that the compressed glass never becomes very hot and recombines strongly during expansion, whereas the hot outer layers expand rapidly before they have a chance to undergo recombination.

We have made an attempt to measure the charge of the late ion pulse by a constant voltage single-detector electrostatic mass spectrometer. In this arrangement, ions of a single charge-to-mass ra-

tio are detected at a given time. The inset in Fig. 3(b) is a typical result showing  $O^{+2}$  ions appearing approximately at the peak of the late ion pulse and a possible pulse of  $O^{+1}$  ions appearing slightly later. In order to determine the exact charge composition of the late pulse, one would have to go through the tedious task of comparing shots with different electric fields in the mass spectrometer and with the same velocity of the later ion pulse. We intend, however, to measure the ion charge and energy spectrum by a multidetector, varying-voltage mass spectrometer.<sup>6</sup> Also, the energy of neutrals within the late pulse is sufficient to allow a secondary emission measurement so that the full current [Fig. 3(a)], rather than just its ionized component, can be detected.

It should be noted that the experimental conditions and results reported here are in sharp contrast to the high-gain, optimized computational results presented elsewhere.<sup>1,7,8</sup> These high-gain results depend on achieving large compressions via especially designed laser pulses which maintain near adiabatic conditions through the dynamics. In such cases, nearly 90% of the mass is ablated and hydrodynamic efficiencies between 5 and 10% are obtained. Here we have used untuned pulses from our current laser configuration, which results in less than 20% of the shell mass being ablated with correspondingly low hydrodynamic efficiencies. What has been observed (Fig. 2) is that for this given configuration, the energy in compression does maximize for some value of the energy absorbed.

To sum up, we have established a simple diagnostic method which can be used to measure the hydrodynamic efficiency in laser-imploded targets for the first time. Only the basic hydrodynamic equations in the code are required to produce the late peak. However, the velocity, charge state, and intensity depend on the precise physical coefficients used to determine the ionization state of the plasma. Comparing measured and computed late peak results then serves as a check of these parameters. The hydrodynamic energy at 10 J absorbed is 0.3 J according to prediction

[Fig. 2(a)]. We get the same result to within a factor of 2 from the experiment if we assume the measured current to be isotropic and derive the mass associated with the late ion pulse as the difference between the initial target mass and that associated with the main ion pulse. This amount of energy would raise a 10-atm fill of deuterium gas to a temperature of 3 keV. However, a core temperature of only  $\sim 1$  keV is derived from the filtered images obtained with an x-ray pinhole camera.<sup>9</sup> Thus, only part of the hydrodynamic energy heats the enclosed gas, while the rest is stored as internal energy in the compressed gas and shell.

This work is supported by the Laser Fusion Feasibility Project of University of Rochester. One of us (E.B.G.) acknowledges partial support under National Science Foundation Grant No. 5-28540 with the Laboratory for Laser Energetics.

---

\*Permanent address: Soreq Nuclear Research Center, Yavne 70600, Israel.

<sup>1</sup>K. A. Brueckner and S. Jorna, *Rev. Mod. Phys.* **46**, 325 (1974).

<sup>2</sup>M. Lubin *et al.*, *Plasma Fusion and Controlled Nuclear Fusion Research* (International Atomic Energy Agency, Vienna, 1975), Vol. II, p. 459; J. Soures, L. M. Goldman, and M. Lubin, *Nucl. Fusion* **13**, 829 (1973).

<sup>3</sup>B. H. Ripin *et al.*, *Phys. Rev. Lett.* **34**, 1313 (1975); G. Charatis *et al.*, *Plasma Fusion and Controlled Nuclear Fusion Research* (International Atomic Energy Agency, Vienna, 1975), Vol. II, p. 250; J. T. Larsen, Lawrence Livermore Laboratory Report No. UCRL-77040, 1975 (unpublished).

<sup>4</sup>E. B. Goldman, *Plasma Phys.* **15**, 289 (1973), and University of Rochester Laboratory for Laser Energetics Report No. 16, 1974 (unpublished).

<sup>5</sup>B. Yaakobi, unpublished.

<sup>6</sup>I. Pelah, M. Oron, and H. Zmora, University of Rochester Laboratory for Laser Energetics Report No. 34, 1976 (unpublished).

<sup>7</sup>J. Nuckolls, L. Wood, A. Thiessen, and G. Zimmerman, *Nature (London)* **239**, 139 (1972).

<sup>8</sup>J. S. Clarke, H. N. Fisher, and R. J. Mason, *Phys. Rev. Lett.* **30**, 89 (1973).

<sup>9</sup>B. Yaakobi *et al.*, to be published.